ISSN (Print) 1226-1750
ISSN (Online) 2233-6656
Journal of Magnetics 25(2), 210-214 (2020) https://doi.org/10.4283/JMAG.2020.25.2.210

The Effect of Fe and Metalloid Contents on Magnetic Properties of Fe–Si–B–P Amorphous Alloys Containing Fe in the Range of 83-85 at%

Mingqing Zuo and Seonghoon Yi*

Department of Materials Science and Metallurgical Engineering, Kyungpook National University, Daegu 41566, Republic of Korea

(Received 1 February 2020, Received in final form 22 April 2020, Accepted 23 April 2020)

A series of Fe–Si–B–P amorphous alloys with high Fe content in the range of 83-85 at.% were successfully prepared through a melt-spinning technique. The effects of Fe content and metalloid elements on thermal and magnetic properties of Fe–Si–B–P amorphous alloys were studied. The saturation magnetization (M_s) values of amorphous alloys tend to decrease with the increase of Fe content higher than 83 at%. For a given Fe content, the replacement of Si or B by P results in a decrease of the M_s value. When the P content more than 5 at.%, the M_s value of the ribbon rapidly decreases. In addition, the compositional dependence of the thermal and magnetic properties has been discussed.

Keywords : Fe–metalloid amorphous alloy, high Fe content, thermal properties, magnetic properties

1. Introduction

As a functional material, soft magnetic materials play an essential role in the field of magnetism and electricity, such as electric motors, power supply transformer and shielding materials [1, 2]. Compared to the conventional widely used Si-steel, Fe-based amorphous alloys exhibit excellent magnetic properties, such as higher effective permeability, lower coercivity, lower hysteresis loss and core loss [3, 4], but nonetheless, Fe-based amorphous alloys possess relatively lower saturation magnetization (M_s) (most are lower than 1.65 T) [5, 6], which restricts their extensive application. So, how to further improve M_s of Fe-based amorphous alloys becomes a hot topic of research.

In the past few decades, hundreds of Fe-based amorphous alloys compositions have been explored, mainly Fe–metalloid based, Fe–TM–metalloid based amorphous alloys (metalloid elements, such as P, B, C, Si; TM is transition metal elements, such as Co, Ni, Mo, Nb) [7-12]. However, the increasing of glass formation ability with adding metal element is usually at the expense of the M_s and cost. Therefore, the development of Fe-based amorphous alloys with high M_s and adequate glass formation ability is tremendously desired. As we all know, the magnetic properties of Fe-based amorphous alloys are mainly contributed by the magnetic moment of the Fe element. We can speculate that the M_s can be improved by increasing the Fe content. On the other hand, the metalloid elements content can also effectively improve the M_s. Therefore, in this work, we have prepared a series of Fe–Si–B–P amorphous alloys with higher Fe content of more than 83 at.%, and the effect of Fe content and metalloid elements (Si, B and P) on the thermal and magnetic properties of Fe–Si–B–P amorphous alloys can be studied.

2. Experimental Methods

Fe–Si–B–P ingots were prepared by arc-melting of high-purity Fe powders (99.9 wt.%), Si pieces (99.9 wt.%), B pieces (99.9 wt.%) and Fe_3P ingots (99.9 wt.%, consisting of 75 at.% Fe and 25 at.% P) under a high-purity argon atmosphere. The amorphous alloy ribbons of 20-25 μm thickness and ~1 mm width were prepared by single roller melt-spinning under a high-purity argon atmosphere (roller speed 40 m s^{-1}). The ribbon structure was identified by X-ray diffraction (XRD, Rigaku D/Max–2500, Japan) with Cu–Kα radiation. The thermal behavior of as–prepared specimens was examined by differential scanning calorimetry (DSC, Perkin Elmer Diamond, USA) at a heating rate of 0.67 K/s under an Ar atmosphere. The magnetic properties of as–quenched specimens were analyzed by vibrating–sample magnetometer (VSM, Lake

*Corresponding author: Tel: +82-53-950-5561
Fax: +82-53-950-6559, e-mail: yish@knu.ac.kr

Table 1. Thermal properties and magnetic properties of the as– quenched Fe–Si–B–P amorphous alloys.

	Composition	Fe content (wt.%)	Phase	Density (g/cm^3)	T_c (K)	T_{x1} (K)	T_{x2} (K)	ΔT (K)	M_s (emu/g)	H_c (A/m)	ΔH (J/g)
#1	$Fe_{85}Si_3B_{10}P_2$	94.92	Am	7.54	569	693	827	135	177.05	27	137
#2	$Fe_{85}Si_3B_8P_4$	94.16	Am	7.45	564	689	817	128	176.53	31	130
#3	$Fe_{85}Si_3B_6P_6$	93.41	Am	7.46	559	679	802	124	173.50	28	125
#4	$Fe_{84}Si_5B_8P_3$	93.62	Am	7.47	591	706	836	130	176.44	34	121
#5	$Fe_{84}Si_5B_6P_5$	92.87	Am	7.42	587	695	820	126	176.76	39	114
#6	$Fe_{84}Si_3B_{10}P_3$	94.27	Am	7.51	587	715	810	95	178.14	28	132
#7	$Fe_{84}Si_3B_8P_5$	93.51	Am	7.47	584	712	803	92	177.00	26	129
#8	$Fe_{84}Si_3B_6P_7$	92.76	Am	7.44	575	701	796	95	173.69	27	125
#9	$Fe_{83}Si_5B_{10}P_2$	93.72	Am	7.47	610	731	833	102	183.64	35	136
#10	$Fe_{83}Si_5B_8P_4$	92.96	Am	7.45	607	726	826	100	182.18	48	126
#11	$Fe_{83}Si_3B_{12}P_2$	94.38	Am	7.50	607	737	805	68	186.66	68	117
#12	$Fe_{83}Si_3B_6P_8$	92.11	Am	7.42	591	717	782	65	183.64	26	120

*Am: Amorphous

Shore 7404 USA) with an applied magnetic field of 1200 kA/m at room temperature.

3. Results and Discussion

In order to investigate the effects of Fe and metalloid element (Si, B and P) contents on thermal and magnetic properties of Fe–Si–B–P amorphous alloys, the compositions listed in Table 1 are studied. Fig. 1 shows the XRD patterns of the as–quenched Fe–Si–B–P ribbons revealing only a broad smooth peak around 2θ–45°and no obvious crystalline peaks can be observed. These XRD patterns are the typical amorphous nature of these specimens. That is, the amorphous phase formation in the ribbons with Fe contents up to 85 at% is possible in this alloy system. Crystalline phases are formed in the ribbons with the Fe content higher than 85 at%.

The DSC thermal scans of the as–quenched amorphous ribbons at a heating rate of 0.67 K/s are shown in Fig. 2. Two exothermal peaks (ΔH) were observed on the DSC curves indicating multi–stage crystallization process. The Curie temperature (T_c), the onset of primary crystallization

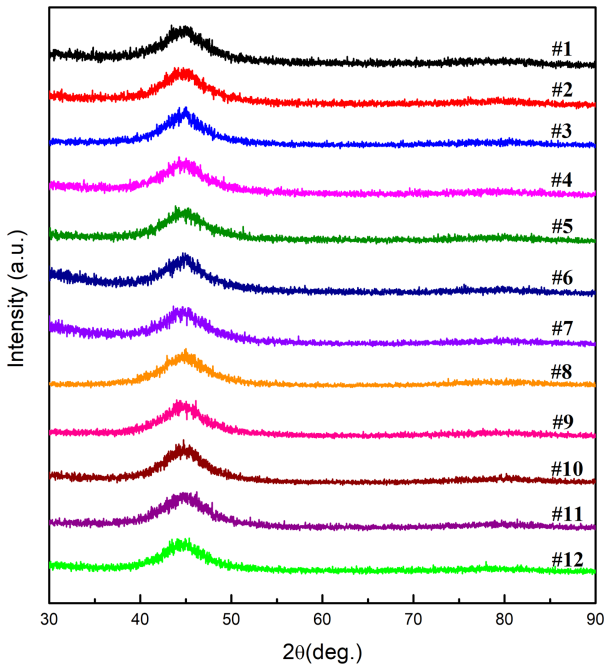

Fig. 1. (Color online) XRD patterns of the as–quenched Fe–Si–B–P amorphous alloys.

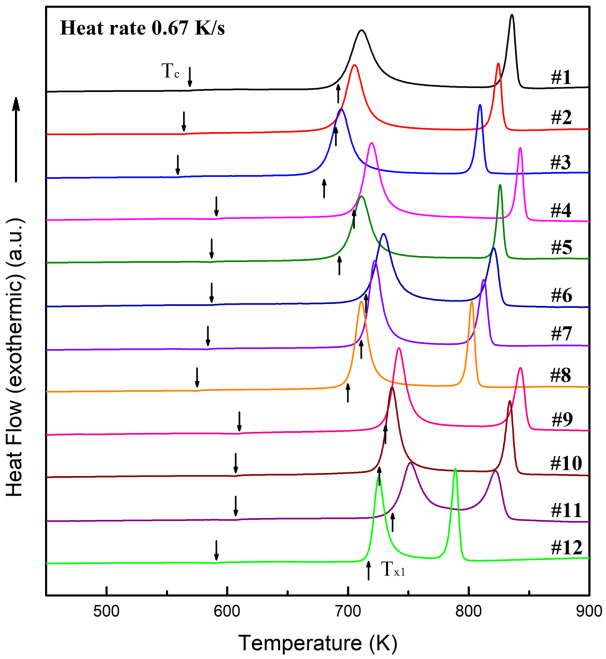

Fig. 2. (Color online) DSC thermal scans of the as–quenched Fe–Si–B–P amorphous alloys.

temperature (T_{x1}) and the onset of secondary crystallization temperature (T_{x2}) of the specimens can be determined from the DSC thermal scans and are summarized in Table 1. In addition, the temperature difference between the onset temperatures of primary crystallization event and secondary crystallization event ($\Delta T = T_{x2} - T_{x1}$) is also summarized in Table 1, which is an important parameter in the fabrication of a nanocrystalline soft magnetic alloy [13]. It can be seen from Table 1 that T_{x1} decrease with increasing the Fe content from 83 to 85 at%. As we know that the onset crystallization temperature of amorphous alloys mainly depends on the atomic bonding strength among the constitution elements [14]. In general, the heat of mixing (ΔH^{mix}) values of Fe–metalloid (Si, B, P and C) atomic pairs are negative values indicating those Fe–metalloid atomic pairs have stronger atomic bonding strength than that of Fe–Fe atomic pair. As the Fe content increases, the number of Fe–metalloid atomic pair decreases reducing the atomic bonding strength of the system and thus, lowers T_{x1}. Therefore, ribbons with high Fe contents tend to exhibit large ΔT ranges. Since the ΔH^{mix} are –35 kJ/mol, –26 kJ/mol and –39.5 kJ/mol for Fe–Si, Fe–B and Fe–P atomic pairs, respectively [15], it can be expected that the replacement of Si or B by P and B by Si may increase the atomic bonding strength of the system, and thus may result in the increase of T_{x1}. However, the experimental results indicate that the substitution of P or Si for B leads to the decrease of T_{x1} in contradiction with the above discussion. In fact, the first–principle simulation result indicates that, except the center site, a considerable number of P atoms can substitute the position of Fe atoms and locate on the shell of the solute–centered atomic cluster. In this situation, excess P atoms tend to form P–Si and P–B atomic pairs reducing Fe–Si and Fe–B atomic pairs [16]. Since the ΔH^{mix} of P–Si (–25.5 kJ/mol) and P–B (0.5 kJ/mol) atomic pairs are less than those of Fe–Si and Fe–B atomic pairs, the replacement of B by P may results in a decrease of atomic bonding strength in the system lowering T_{x1} of the ribbon. However, a detailed study on the atomic cluster structure is required to clearly verify this issue.

Figure 3(a), 3(b) and 3(c) present the hysteresis loops of the as–quenched ribbons at room temperature, respectively. The inset depicts the enlarged partial curves of the hysteresis loops. All the samples exhibit typical soft magnetic properties. The saturation magnetization (M_s) of the specimens is determined from the hysteresis loops and summarized in Table 1. The M_s value of the $Fe_{83}Si_3B_{12}P_2$ amorphous ribbon is 1.76 T. In general, the M_s values of Fe-based amorphous ribbons tend to increase as the Fe content of ribbon increases. However, the M_s value

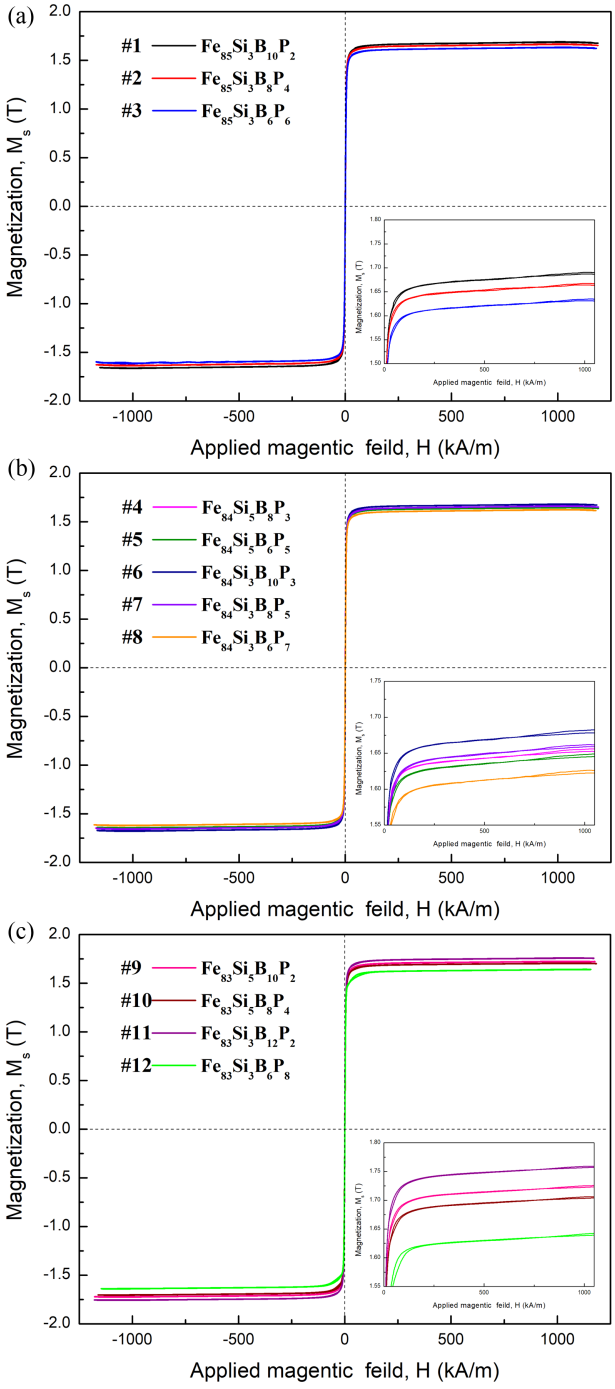

Fig. 3. (Color online) Hysteresis loops of the as–prepared (a) $Fe_{85}(SiBP)_{15}$, (b) $Fe_{84}(SiBP)_{16}$ and (c) $Fe_{83}(SiBP)_{17}$ ribbons at room temperature. The inset depicts the enlarged partial curves of the hysteresis loops.

decreases with further increase of the Fe content up to 85 at% in this study. Luborsky [17] and Kong *et al.* [18] reported similar results, which indicates that the M_s value first increase and then decrease with the increase of Fe content at room temperature in the Fe–metalloid amorph-

ous system. Moreover, it is known that the band splitting is due to the exchange interaction of the band electrons, and the stronger exchange interaction leads to the larger split between spin–up (majority) and spin–down (minority) bands. For the Fe–Si–B–P system, the split of the 3*d* bands decreases with higher Fe content due to the weaker exchange interaction between Fe atoms, which reduces the magnetic moment of Fe atoms. On the other hand, as shown in Table 1, for a given Fe content, the M_s of Fe–Si–B–P amorphous ribbons decrease with the substitution of P for Si or B and Si for B. As we know, M_s of an alloy arises from the magnetic moment of its composing atoms, the magnetic moment of transition metal can be attributed to the unpaired electron spins. Based on the charge transfer model [19, 20] and rigid–band model [21], for Fe–metalloid amorphous alloys, the valence elements, i.e. *sp* electrons, of metalloid elements will transfer to the 3*d* minority–spin band of Fe atom, leading to decrease of the magnetic moment, thus reducing the M_s of Fe–metalloid amorphous alloys. The number of *sp* electrons of P, Si and B atoms is 5, 4 and 3, respectively. Thus, the replacement of Si or B by P with more *sp* electrons results in a decrease of saturation magnetization in Fe–Si–B–P system. It is worth noting that M_s rapidly decreases when the P content more than 5 at.%, which indicates too many P will leads to worsening saturation magnetization.

The Curie temperature (T_c) is also an essential parameter of magnetic properties and identified in Table 1. It is seen that the T_c decrease with increasing the Fe content from 83 at.% to 85 at.%. Moreover, replacement of Si by P or B and B by P will also decrease of T_c when given Fe content. According to the mean field theory, the Curie temperature is proportional to exchange integral between magnetic atoms and average spin moment of magnetic atoms [22]. It is well known that the position of Fe on the Bethe–slater curve lies on the left side of the maximum. So the larger average atomic distance between Fe atoms will result in the stronger exchange interaction between Fe atoms, and thus increasing the T_c. Therefore, more increase of Fe content will leads to the reduction in the average distance between Fe–Fe atoms, and then result in the weaker atomic exchange interaction, thus lower T_c. The atomic radius of P, Si and B is 0.109 nm, 0.117 nm and 0.09 nm, respectively [15]. Compared with P and B, Si atom has a larger atomic radius. So it explained that the substitution of Si for P or B will leads to the larger average atomic distance between Fe atoms, and the stronger atomic exchange interaction between Fe atoms, resulting in a higher T_c. The radius of P atom is larger than B atom, it seems that replacing B with P can increase the average atomic distance between Fe atoms increase the exchange interaction, and leads to the increase of T_c. However, the experiment results are contrary to expectations. In previous studies [11], it is shown that the substitution of P for B will reduce the average atomic distance between Fe atoms and reduce the exchange interaction, resulting in lower T_c. Therefore, the T_c of Fe–rich of Fe–Si–B–P system will reduce with replacing Si with P or B and B with P.

4. Conclusion

We systematically investigated the thermal stability and magnetic properties of Fe–Si–B–P amorphous alloys with high Fe contents from 83 at.% to 85 at.% and different contents of metalloids. The results show it has a high saturation magnetization of more than 1.7 T when the Fe content is 83 at%. At the same time, it also has high thermal stability. Excessively high Fe content of the ribbon may lead to decrease of T_c, T_{x1} and saturation magnetization. Thus, it proves that Fe–rich amorphous alloys are not conducive to the improvement of magnetic properties. For a given Fe content, the replacement of P by Si and B by P or Si lead to decrease of T_{x1}. The substitution of P or B for Si and P for B will decrease of T_c.

Acknowledgements

This study was supported financially by the Civil-Military Technology Cooperation Program (18-CM-MA-15) of Defense Acquisition Program Administration.

References

[1] R. C. O'handley, Modern magnetic materials: principles and applications, Wiley, 2000.
[2] J. Zhang, J. Li, G. Tan, R. Hu, J. Wang, C. Chang, and X. Wang, ACS Appl. Mater Interfaces **9**, 42192 (2017).
[3] A. Inoue, Materials Science and Engineering: A **226**, 357 (1997).
[4] A. Inoue, A. Takeuchi, and B. Shen, Mater. Trans. **42**, 970 (2001).
[5] Y. A. Yoshizawa, S. Oguma, and K. Yamauchi, J. Appl. Phys. **64**, 6044 (1988).
[6] A. Makino, C. Chang, T. Kubota, and A. Inoue, J. Alloys and Compd. **483**, 616 (2009).
[7] J. Y Hwang, H. S. Lee, and S. Yi, Metals and Mater. International **25**, 1 (2019).
[8] B. Shen, M. Akiba, and A. Inoue, Physical Review B **73**, 104204 (2006).
[9] P. Tiberto, R. Piccin, N. Lupu, H. Chiriac, and M. Baricco, J. Alloys and Compd. **483**, 608 (2009).
[10] B. Shen, M. Akiba, and A. Inoue, Appl. Phys. Lett. **88**,

131907 (2006).
[11] M. Zuo, S. Meng, Q. Li, H. Li, C. Chang, and Y. Sun, Intermetallics **83**, 83 (2017).
[12] Q. Li and S. Yi, Metals and Materials International **20**, 7 (2014).
[13] J. Wang, Z. Wang, Y.-y. Jia, R.-m. Shi, Z.-p. Wen, and H.-j. Kang, J. Appl. Phys. **113**, 17A310 (2013).
[14] H. Chen, Reports on Progress in Physics **43**, 353 (1980).
[15] A. Takeuchi and A. Inoue, Mater. Trans. **46**, 2817 (2005).
[16] W. Zhang, Q. Li, and H. Duan, J. Appl. Phys. **117**, 104901 (2015).
[17] F. Luborsky, IEEE Trans. Magn. **14**, 1008 (1978).
[18] F. Kong, C. Chang, A. Inoue, E. Shalaan, and F. Al-Marzouki, J. Alloys and Compd. **615**, 163 (2014).
[19] K. Yamauchi and T. Mizoguchi, Journal of the Physical Society of Japan **39**, 541 (1975).
[20] K. Schwarz and D. R. Salahub, Physical Review B **25**, 3427 (1982).
[21] Y. Kakehashi, Modern Theory of Magnetism in Metals and Alloys, Springer Science & Business Media (2013).
[22] B. D. Cullity and C. D. Graham, Introduction to magnetic materials, John Wiley & Sons (2011).